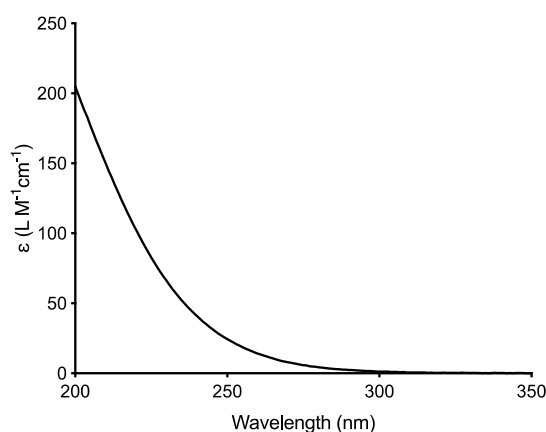


34 **1 Fluence determination**

35

36 Fluence was determined for MPUV and LPUV irradiation experiments following
37 standardized methods where UV fluence is calculated by multiplying the average irradiance by
38 the exposure time in seconds.¹ The average irradiance was determined by correcting the incident
39 irradiance (radiometer reading) for sample depth, absorbance, sample reflectance, petri factor
40 and sensor factor (MPUV only). This method for MPUV fluence determination is herein defined
41 as “unweighted.” If the sample contained H₂O₂ and irradiated with MPUV, an H₂O₂-weighted
42 fluence method ² was applied, unless noted otherwise, which follows the method described
43 above ¹ and also weights each wavelength by the H₂O₂ molar absorption spectrum relative to its
44 value at 254 nm.

45 As noted in Bircher (2015) ², H₂O₂ weighted fluence is similar to DNA weighted fluence.
46 The difference between the two methods is that H₂O₂ weighted fluence values are weighted by
47 the H₂O₂ molar absorption spectrum (200 – 350 nm) (Figure S1) relative to its value at 254 nm,
48 whereas DNA weighted fluence values are weighted by the germicidal (DNA) absorption
49 spectrum or action spectra of a target microorganism relative to its value at 254 nm.
50



51

52 Figure S1. Molar absorbance spectra of H₂O₂.

53

54 The selected fluence calculation method will influence sample irradiation times that are
 55 needed to achieve a target fluence. For instance, irradiation times determined by H₂O₂ and DNA
 56 weighted fluence methods will be relatively lower for a given fluence in waters with low
 57 absorbance at < 240 nm and 260 nm, respectively, since H₂O₂ and DNA absorb photons of light
 58 efficiently at these wavelengths. Table S1 illustrates the different exposure times required to
 59 achieve a fluence level of 1000 mJ/cm² using unweighted, H₂O₂ weighted and DNA weighted
 60 fluence determination methods for two different absorbing waters. As shown, the irradiation
 61 times differ between the applied fluence determination methods and the two waters. Overall,
 62 irradiation times for water 2 are lower than water 1 since it can be assumed that water 2 is a
 63 lower absorbing water matrix (as indicated by its UV absorbance at 200 nm and 254 nm). In
 64 comparing unweighted and H₂O₂ weighted irradiation times, the H₂O₂ weighted irradiation time
 65 is 20% higher than the unweighted irradiation time for water 1. In contrast, the H₂O₂ weighted
 66 irradiation time is 13% lower than the unweighted irradiation time for water 2. This is because
 67 the absorbance at 200 nm of water 1 is relatively high compared to water 2.

68
 69 Table S1. A relative comparison of MPUV irradiation times for two waters using unweighted,
 70 H₂O₂ weighted and DNA weighted fluence determination methods. UV absorbance (UVA)
 71 values are provided at 200 nm and 254 nm. Irradiation times reflect the exposure time needed to
 72 achieve a fluence level of 1000 mJ/cm².

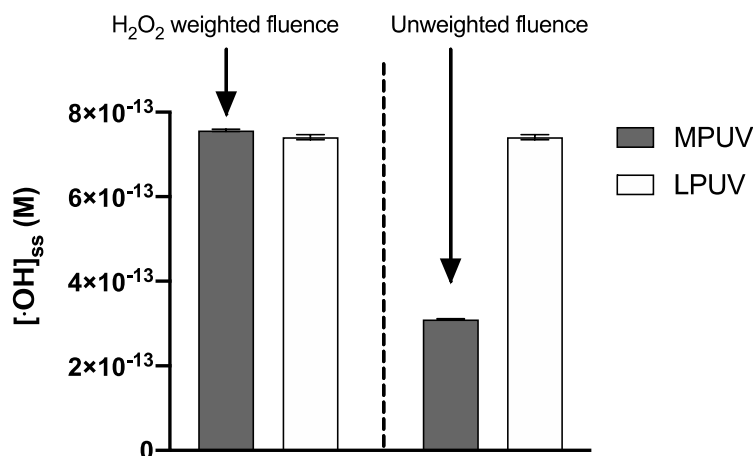
Fluence determination method	Water 1	Water 2
	UVA 200 = 0.094 cm ⁻¹ UVA 254 = 3.2 cm ⁻¹	UVA 200 = 0.007cm ⁻¹ UVA 254 = 1.2 cm ⁻¹
	Irradiation time (sec)	
Unweighted	765	540
H ₂ O ₂ weighted	931	475
DNA weighted	1103	789

74
 75 An advantage of applying H₂O₂ weighted fluence instead of unweighted fluence is that
 76 compound degradation rates achieved during MPUV experiments can be directly compared to

77 those achieved during LPUV experiments, assuming water quality and experimental conditions
78 remain constant. To validate this point, separate experiments were performed. Deionized water
79 (0 mg-N/L of nitrate and nitrite) containing ~1 mg/L of pCBA and 10 mg/L H₂O₂ was irradiated
80 with MPUV and LPUV (1000 mJ/cm²). MPUV exposure times were determined by H₂O₂
81 weighted and unweighted fluence methods. Hydroxyl radical steady concentrations ([·OH]_{ss})
82 were used as a metric to compare results, and [·OH]_{ss} calculations followed methods presented in
83 Keen et al. (2012) ³.

84 The results are presented in Figure S2. When H₂O₂ weighted fluence was used to
85 determine MPUV irradiation times, the [·OH]_{ss} were comparable between MPUV and LPUV.
86 However, MPUV irradiation times determined using unweighted fluence yielded [·OH]_{ss} values
87 that were approximately two times lower than LPUV [·OH]_{ss} values.

88



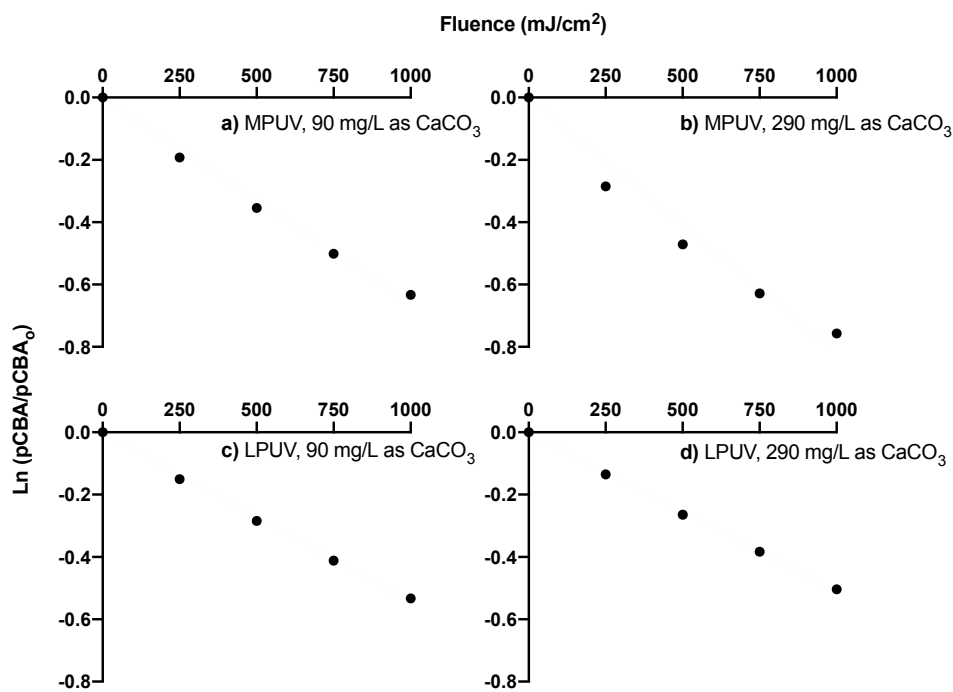
89
90 Figure S2. Comparison of hydroxyl radical steady state concentrations ([·OH]_{ss}) determined for
91 MPUV and LPUV irradiation (1000 mJ/cm²) of deionized water containing pCBA (1 mg/L) and
92 10 mg/L of H₂O₂. For MPUV, [·OH]_{ss} values were determined using H₂O₂ weighted fluence (left
93 side) and unweighted fluence (right side). LPUV [·OH]_{ss} values are the same on both sides of the
94 graph. Error bars represent the standard deviation between duplicate experiments.

95
96

97 **2 Central composite design**

98

99 A central composite design (CCD) was utilized to systematically evaluate the significance of
100 nitrate, H₂O₂ and alkalinity concentration (Tables S2) on radical production during MPUV and
101 LPUV irradiation experiments (1000 mJ/cm²). pCBA degradation rates (k'_{pCBA}) were used to
102 indirectly measure the production of radicals in irradiated synthetic water that contained
103 Suwannee River Fulvic Acid (SRFA) as the dissolved organic carbon (DOC) source (Table 2 in
104 the manuscript). Pseudo first order degradation plots of pCBA were found to exhibit first order
105 behavior (Figure S3). The central composite design experimental matrix was comprised of a total
106 of 38 experiments (19 experiments and 5 center points per lamp type, Table S2). k'_{pCBA} values
107 are provided in Table S2.



108

109 Figure S3. MPUV (top row) and LPUV (bottom row) pseudo first order pCBA degradation plots
110 of measured pCBA in SRFA synthetic water (Table 2 within the manuscript) containing low (90
111 mg/L as CaCO₃, plots a and c) and high (290 mg/L as CaCO₃, plots b and d) alkalinity. Nitrate
112 (10 mg-N/L) and H₂O₂ (3 mg/L) concentrations remained constant.
113

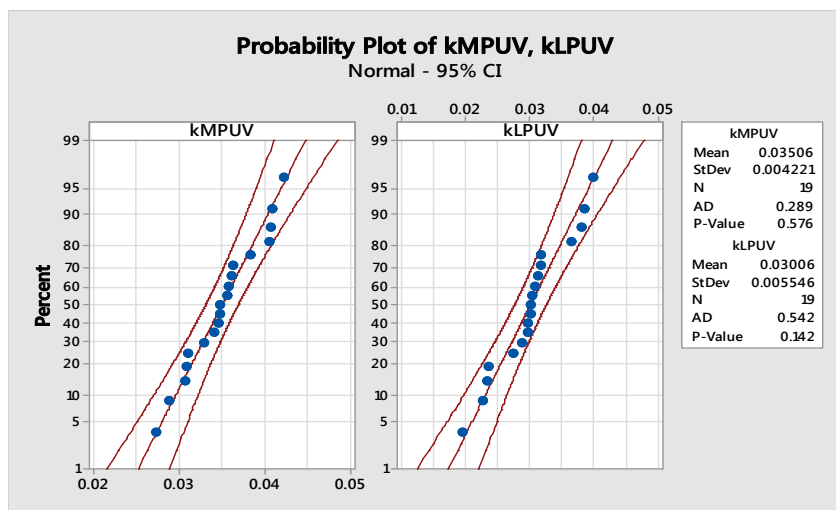
114 **2.1 Central composite design analysis**

115

116 Minitab Software, version 17 (Minitab LLC, PA) was used to evaluate the effect of the
117 independent factors (i.e., nitrate, H₂O₂ and alkalinity concentration) and the response (k'_{pCBA} and
118 nitrite). The response was transformed using a power transformation (i.e., (k'_{pCBA})^{1/2}) to stabilize
119 the variance and improve model fit ⁴. All experiments (Table S2 and S6) were performed in
120 random order. MPUV and LPUV transformed k'_{pCBA} values were found to be normally
121 distributed (p values > 0.05) (Figure S4), therefore, the null hypothesis that the data is not
122 normally distributed cannot be rejected.

123

124



125

126 Figure S4. Probability plots generated in Minitab illustrating normal distribution of transformed
127 pCBA degradation rates, (k'_{pCBA})^{1/2}, obtained for MPUV (left plot) and LPUV (right plot)
128 irradiation experiments (Table S2).

129

130

131

132

133

134

135

136

137

138 Table S2. Experimental central composite design (CCD) and corresponding pCBA pseudo first
 139 order degradation results (k'_{pCBA}) for MPUV and LPUV. k'_{pCBA} values were determined for a
 140 UV fluence up to 1000 mJ/cm². Experiments were run in random order and in SRFA synthetic
 141 water (Table 2 within the manuscript). Transformed data, i.e. $(k'_{pCBA})^{1/2}$, were used for CCD
 142 analysis.

143

Exp. ID	Variables			MPUV k'_{pCBA} (cm ² /mJ)	LPUV k'_{pCBA} (cm ² /mJ)	Transformed	
	NO ₃ ⁻ (mg-N/L)	H ₂ O ₂ (mg/L)	Alkalinity (mg/L as CaCO ₃)			MPUV k'_{pCBA}	LPUV k'_{pCBA}
1	3	3	90	1.09E-03	8.24E-04	3.30E-02	2.87E-02
2	10	3	90	1.16E-03	5.45E-04	3.40E-02	2.33E-02
3	3	8	90	1.66E-03	1.59E-03	4.08E-02	3.98E-02
4	10	8	90	1.79E-03	1.44E-03	4.23E-02	3.80E-02
5	3	3	290	7.46E-04	5.36E-04	2.73E-02	2.32E-02
6	10	3	290	9.43E-04	5.09E-04	3.07E-02	2.26E-02
7	3	8	290	1.20E-03	1.00E-03	3.46E-02	3.17E-02
8	10	8	290	1.47E-03	9.96E-04	3.84E-02	3.16E-02
9	0.6	5.5	190	9.60E-04	9.02E-04	3.10E-02	3.00E-02
10	12.4	5.5	190	1.31E-03	8.97E-04	3.62E-02	3.00E-02
11	6.5	1.3	190	8.27E-04	3.68E-04	2.88E-02	1.92E-02
12	6.5	9.7	190	1.64E-03	1.48E-03	4.05E-02	3.85E-02
13	6.5	5.5	22	1.66E-03	1.33E-03	4.08E-02	3.64E-02
14	6.5	5.5	358	9.47E-04	7.46E-04	3.08E-02	2.73E-02
15	6.5	5.5	190	1.21E-03	9.08E-04	3.48E-02	3.01E-02
16	6.5	5.5	190	1.21E-03	8.78E-04	3.48E-02	2.96E-02
17	6.5	5.5	190	1.28E-03	8.68E-04	3.58E-02	2.95E-02
18	6.5	5.5	190	1.30E-03	9.38E-04	3.61E-02	3.06E-02
19	6.5	5.5	190	1.27E-03	9.64E-04	3.56E-02	3.10E-02

144
 145
 146
 147
 148
 149
 150
 151
 152
 153
 154
 155
 156
 157
 158
 159
 160

161 Table S3. Corresponding pH values for the central composite design (CCD) results (Table S2).

Exp. ID	Variables			MPUV		LPUV	
	NO ₃ ⁻ (mg-N/L)	H ₂ O ₂ (mg/L)	Alkalinity (mg/L as CaCO ₃)	pH (SU)			
				Initial	Final	Initial	Final
1	3	3	90	8.5	8.7	8.5	8.7
2	10	3	90	8.5	8.7	8.5	8.5
3	3	8	90	8.5	8.5	8.5	8.6
4	10	8	90	8.5	8.6	8.5	8.6
5	3	3	290	8.5	8.7	8.5	8.4
6	10	3	290	8.5	8.6	8.5	8.7
7	3	8	290	8.5	8.6	8.5	8.7
8	10	8	290	8.5	8.4	8.5	8.5
9	0.6	5.5	190	8.6	8.4	8.6	8.3
10	12.4	5.5	190	8.6	8.5	8.6	8.4
11	6.5	1.3	190	8.6	9.1	8.6	8.7
12	6.5	9.7	190	8.6	8.7	8.6	9
13	6.5	5.5	22	8.6	8.6	8.6	8.3
14	6.5	5.5	358	8.6	8.7	8.6	8.7
15	6.5	5.5	190	8.6	8.6	8.6	8.6
16	6.5	5.5	190	8.6	9.1	8.6	8.6
17	6.5	5.5	190	8.6	8.8	8.6	8.5
18	6.5	5.5	190	8.6	8.5	8.6	8.5
19	6.5	5.5	190	8.7	8.6	8.7	8.4

162

163

164 **2.2 Model adequacy**

165

166 The significance of model terms on the response was evaluated at a 90% confidence level

167 using analysis of variance (ANOVA). For ANOVA, significant terms exhibited an F-value that

168 was higher than the critical F-values for a given degrees of freedom and a p-value < 0.1. A

169 stepwise backwards elimination approach was applied to remove the least significant terms from

170 the quadratic model until all variables in the model had a p-value less than or equal to the alpha

171 value set at 0.1. The ANOVA results are presented in Table S3.

172 Model adequacy was further evaluated by performing a residual versus fits analysis

173 (Figure S5). As shown in Figure S5, data is randomly scattered about the 0 y-axis indicating the

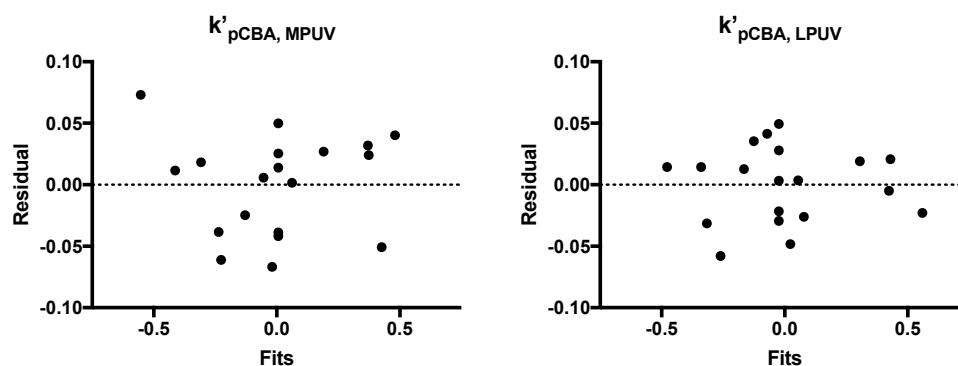
174 model is a good fit.

175

176 Table S4. ANOVA table for MPUV (left) and LPUV (right) k'_{pCBA} response surface quadratic
 177 model.

MPUV k'_{pCBA}				LPUV k'_{pCBA}			
Source	DF	F-Value	P-Value	Source	DF	F-Value	P-Value
Model	5	138	0	Model	7	93	0
Linear	3	225	0	Linear	3	209	0
NO ₃ ⁻	1	55	0	NO ₃ ⁻	1	5.7	0.036
H ₂ O ₂	1	413	0	H ₂ O ₂	1	505	0
Alkalinity	1	206	0	Alkalinity	1	116	0
Square	1	9.0	0.010	Square	2	5.5	0.022
(NO ₃ ⁻) ²	1	9.0	0.010	(H ₂ O ₂) ²	1	4.8	0.052
				(Alkalinity) ²	1	4.9	0.049
2-Way Interaction	1	5.9	0.030	2-Way Interaction	2	8.3	0.006
NO ₃ ⁻	1	5.9	0.030	NO ₃ ⁻	1	6.3	0.029
× Alkalinity				× Alkalinity			
				H ₂ O ₂ × Alkalinit	1	10	0.008
Error	13			Error	11		
Lack-of-Fit	9	1.4	0.394	Lack-of-Fit	7	2.4	0.211
Pure Error	4			Pure Error	4		
Total	18			Total	18		

178
 179



180
 181 Figure S5. Residual versus fits analysis for dimensionless response variables k'_{pCBA} MPUV (left)
 182 and k'_{pCBA} LPUV (right).

183
 184 The significant model terms are presented in equations 1 and 2. The squared alkalinity
 185 term, found to be significant via ANOVA analysis (Table S4, LPUV), was not included in
 186 equation 2 because the value was an order of magnitude lower than other significant terms. With

187 the exception of the $(H_2O_2)^2$ term in eq. 2, all main and interaction terms (eq. 1 and 2) had a p-
 188 value < 0.05 (Table S4).

189

$$(k'_{pCBA} MPUV)^{\frac{1}{2}} = 2.99 \times 10^{-2} + (6.4 \times 10^{-4} NO_3) + (1.49 \times 10^{-3} H_2O_2) - (3.70 \times 10^{-5} alkalinity) - (4.40 \times 10^{-5} (NO_3)^2) + (2.00 \times 10^{-6} (NO_3 \times alkalinity))$$

190
 191 (1)
 192

$$(k'_{pCBA} LPUV)^{\frac{1}{2}} = 2.19 \times 10^{-2} - (6.10 \times 10^{-4} NO_3) + (3.94 \times 10^{-3} H_2O_2) - (3.90 \times 10^{-5} alkalinity) - (8.50 \times 10^{-5} (H_2O_2)^2) + (2.00 \times 10^{-6} NO_3 \times alkalinity) - (4.00 \times 10^{-6} (H_2O_2 \times alkalinity))$$

193
 194 (2)
 195
 196

197 2.3 Validation of CCD results

198

199 To validate results found by CCD analysis, separate experiments were performed in SRFA
 200 synthetic water (Table 2 within the manuscript) at a fixed H_2O_2 concentration (10 mg/L) with
 201 high and low alkalinity (60 and 300 mg/L as $CaCO_3$) and nitrate (1 and 10 mg-N/L) (Table S5).

202

203 Table S5. MPUV and LPUV k'_{pCBA} values determined in SRFA synthetic water (Table 2 within
 204 the manuscript) at high and low alkalinity and nitrate concentrations and set H_2O_2 concentration
 205 (10 mg/L). Each k'_{pCBA} value is the average of duplicate experiments (coefficient of variation
 206 was < 6%, n=2).

Alkalinity (mg/L as $CaCO_3$)	MPUV k'_{pCBA} (cm^2/mJ)		LPUV k'_{pCBA} (cm^2/mJ)	
	Nitrate (mg-N/L)			
	1	10	1	10
60	-1.74E-03	-1.83E-03	-2.20E-03	-2.08E-03
300	-1.34E-03	-1.41E-03	-1.42E-03	-1.50E-03

207

208 An increase in nitrate concentration from 1 to 10 mg-N/L at low alkalinity resulted in a ~5%

209 increase and decrease in k'_{pCBA} values for MPUV and LPUV, respectively. At high alkalinity

210 conditions, the same increase in nitrate concentration led to a ~5% increase in k'_{pCBA} values for
 211 both MPUV and LPUV, which aligns with the trends observed in Figure 3 of the manuscript and
 212 further validates CCD findings.

213 3 Experimental matrix

214

215 The experimental matrix presented in Table S2 was supplemented with two additional

216 experiments, 20 and 21. Analysis of the data is discussed in section 4.2 of the manuscript. Table

217 S6 also reports the k'_d as a percent of the overall k'_{pCBA} value for a given test condition.

218

219 Table S6. Experimental matrix and corresponding pCBA pseudo first order degradation results
 220 (k'_{pCBA}) for MPUV and LPUV. Experiments were run in random order and in SRFA synthetic
 221 water (Table 2 within the manuscript). The contribution of direct photolysis (k'_d) to the overall
 222 k'_{pCBA} value is reported and was calculated using $1.37 \times 10^{-4} \text{ cm}^2/\text{mJ} \pm 3\%$ (average followed by
 223 the coefficient of variation, $n=4$) and $1.21 \times 10^{-4} \text{ cm}^2/\text{mJ} \pm 2\%$ for MPUV and LPUV,
 224 respectively.

Exp. ID	NO ₃ ⁻ (mg-N/L)	H ₂ O ₂ (mg/L)	Alkalinity (mg/L as CaCO ₃)	NO ₃ ⁻ /H ₂ O ₂	MPUV k'_{pCBA} (cm ² /mJ)	Contribution of MPUV k'_d	LPUV k'_{pCBA} (cm ² /mJ)	Contribution of LPUV k'_d
1	3	3	90	1.0	1.09E-03	13%	8.24E-04	15%
2	10	3	90	3.5	1.16E-03	12%	5.45E-04	22%
3	3	8	90	0.4	1.66E-03	8%	1.59E-03	8%
4	10	7	90	1.3	1.79E-03	8%	1.44E-03	8%
5	3	4	290	0.8	7.46E-04	18%	5.36E-04	23%
6	10	3	290	3.5	9.43E-04	15%	5.09E-04	24%
7	3	8	290	0.4	1.20E-03	11%	1.00E-03	12%
8	10	8	290	1.3	1.47E-03	9%	9.96E-04	12%
9	1	5	197	0.1	9.60E-04	14%	9.02E-04	13%
10	12	6	197	2.2	1.31E-03	10%	8.97E-04	13%
11	7	1	197	4.4	8.27E-04	17%	3.68E-04	33%
12	7	10	197	0.7	1.64E-03	8%	1.48E-03	8%
13	7	6	30	1.2	1.66E-03	8%	1.33E-03	9%
14	7	6	420	1.2	9.47E-04	15%	7.46E-04	16%
15	7	6	197	1.2	1.21E-03	11%	9.08E-04	13%
16	7	6	197	1.2	1.21E-03	11%	8.78E-04	14%
17	7	6	197	1.2	1.28E-03	11%	8.68E-04	14%
18	7	6	197	1.2	1.30E-03	11%	9.38E-04	13%
19	7	6	197	1.2	1.27E-03	11%	9.64E-04	13%
20	6	2	76	3.5	7.56E-04	18%	3.83E-04	32%

21	6	1	76	4.5	8.90E-04	15%	3.53E-04	34%
----	---	---	----	-----	----------	-----	----------	-----

225

226

227 **4 Nitrate and nitrite concentrations**

228

229 The initial nitrate and final nitrite concentrations after MPUV and LPUV irradiation

230 experiments (Table S2) are presented in Table S7.

231

232 Table S7. Nitrate and nitrite concentrations were measured using the cadmium reduction flow
 233 injection method which is compliant with Standard Method 4500. The detection limit (DL) for
 234 nitrate plus nitrite is 0.004 mg-N/L and nitrite is 0.005 mg-N/L. The initial nitrite concentration
 235 for all experiments was 0 mg-N/L, and final nitrite concentrations were measured after MPUV
 236 and LPUV irradiation up to 1000 mJ/cm².

Exp. ID	Nitrate (mg-N/L)	MPUV, Nitrite (mg-N/L)	LPUV, Nitrite (mg-N/L)	MPUV, NO ₂ ⁻ / NO ₃ ⁻	LPUV, NO ₂ ⁻ / NO ₃ ⁻
1	3	0.22	1.3E-02	7.4%	0.33%
2	10	0.33	3.4E-02	3.2%	0.32%
3	3	0.21	1.1E-02	7.6%	0.37%
4	10	0.28	2.2E-02	2.8%	0.23%
5	3	0.22	9.0E-03	7.4%	0.30%
6	10	0.27	2.6E-02	2.5%	0.25%
7	3	0.22	1.2E-02	8.1%	0.41%
8	10	0.31	2.9E-02	2.7%	0.33%
9	0.6	0.10	DL	14.9%	0.00%
10	12.4	0.33	3.1E-02	2.6%	0.23%
11	6.5	0.29	1.4E-02	4.5%	0.21%
12	6.5	0.29	1.5E-02	4.3%	0.20%
13	6.5	0.26	1.2E-02	3.9%	0.18%
14	6.5	0.28	1.6E-02	4.1%	0.24%
15	6.5	0.23	2.0E-02	3.1%	0.31%
16	6.5	0.28	2.6E-02	4.3%	0.40%
17	6.5	0.24	2.2E-02	3.6%	0.34%
18	6.5	0.27	2.2E-02	4.2%	0.23%
19	6.5	0.25	2.1E-02	3.8%	0.32%

237

238

239

240

241

242
243
244
245

246 **5 Calculations**

247

248 **5.1 OH^\ominus scavenging calculation**

249

250 The scavenging capacity of the water matrices evaluated in Figure 8 within the manuscript
251 was determined by multiplying the second order OH^\ominus rate constant (k_{OH^\ominus} , $\text{M}^{-1}\text{s}^{-1}$) of the
252 scavenger [S] by its measured molar concentration. Literature values of k_{OH^\ominus} are provided in
253 Table S7.

254

255 Table S8. The OH^\ominus scavengers evaluated for Figure 8 within the manuscript and their
256 corresponding second order rate constants with OH^\ominus .

Scavenger	k_{OH^\ominus} ($\text{M}^{-1}\text{s}^{-1}$)	Reference
SRFA DOC	2.06×10^8	McKay et al., 2011 ⁵
NO_2^-	1.00×10^{10}	Buxton et al., 1988 ⁶
HCO_3^-	8.5×10^6	Buxton et al., 1988 ⁶
CO_3^{2-}	3.9×10^8	Buxton et al., 1988 ⁶
H_2O_2	2.70×10^7	Buxton et al., 1988 ⁶

257

258

259

260 **5.2 Molar absorption coefficient calculation**

261

262 Molar absorption coefficient values of H_2O_2 and nitrate were experimentally calculated by
263 applying Beer-Lambert Law (equation 3), where ϵ ($\text{M}^{-1}\text{cm}^{-1}$) is the molar absorption coefficient,
264 A (cm^{-1}) is the sample absorbance at a specific wavelength, c is the molar concentration (M) and
265 l is the optical pathlength (1 cm) (Table S9). Absorbance values were measured using a Cary 100
266 Bio UV-Vis spectrophotometer (Agilent Technologies, CA). Since nitrate absorbs strongly at
267 wavelengths above > 220 nm and weakly at wavelengths < 250 nm, higher and lower nitrate
268 concentrations were used to measure the absorbance at 200 nm and 254 nm, respectively.

$$\varepsilon = \frac{A}{c \times l} \quad (3)$$

269

270

271

272

273 Table S9. Molar concentration (c), absorbance (A) and corresponding molar absorption
 274 coefficient (ε) values for H₂O₂ and nitrate at 200 nm and 254 nm. Absorbance was measured
 275 using a 1 cm cell pathlength.

276

Wavelength (nm)	H ₂ O ₂			Nitrate		
	c (M)	A (cm ⁻¹)	ε (M ⁻¹ cm ⁻¹)	c (M)	A (cm ⁻¹)	ε (M ⁻¹ cm ⁻¹)
200	5.88E-04	0.121	205	7.13E-05	0.718	10066
254	5.88E-04	0.012	20	7.13E-04	0.005	6

277

278 6 MPUV irradiation experiments with nitrified wastewater and groundwater

279

280 Photolysis of nitrate can generate OH^\bullet thereby creating a *de facto* advanced oxidation
 281 process (AOP). OH^\bullet generation by MPUV photolysis of nitrate will occur more efficiently than
 282 OH^\bullet generation by LPUV photolysis of nitrate because nitrate absorbs photons more strongly
 283 at wavelengths < 250 nm. Therefore, a major advantage of MPUV photolysis of nitrate is the
 284 generation of OH^\bullet without oxidant addition.

285 To demonstrate this point, groundwater (collected from a well in Los Angeles, CA) and
 286 nitrified wastewater effluent (Metro Wastewater Reclamation, Denver, CO) that contained native
 287 nitrate concentrations (see Table S10 for water quality data) were spiked with pCBA (1 mg/L)
 288 and irradiated with MPUV (1000 mJ/cm²). The contribution of MPUV direct photolysis (k'_d) to
 289 the total pCBA decay rate (k'_{pCBA}) was subtracted ($k'_{\text{pCBA, indirect}} = k'_{\text{pCBA}} - k'_d$) in order to isolate
 290 pCBA degradation via radical oxidation ($k'_{\text{pCBA, indirect}}$). Values of MPUV $k'_{\text{pCBA, indirect}}$ were then
 291 compared to the theoretical pCBA decay rates that would be achieved by LPUV/H₂O₂. LPUV
 292 k'_{pCBA} values were attained by modeling pCBA degradation following methods presented by
 293 Wols et al. (2013) ⁷.

294 As discussed in section 4 of the manuscript, the pCBA degradation rates (Table S11)
 295 achieved in these systems after 1000 mJ/cm² were equivalent to LPUV irradiation (1000 mJ/cm²)
 296 of the same experimental matrix containing ~1.5 mg/L and ~4 mg/L H₂O₂. It is important to note
 297 that if a MPUV fluence other than 1000 mJ/cm² was applied, the corresponding equivalent H₂O₂
 298 concentration for LPUV would change since nitrite levels after MPUV would be different.

299
 300 Table S10. Water quality data for groundwater and nitrified wastewater effluent. Groundwater
 301 samples were collected from a well site in Los Angeles, CA and wastewater effluent was
 302 collected after biological aeration followed by filtration from Metro Wastewater Reclamation
 303 (Denver, CO). The UV absorbance measured at 254 nm (UVA 254) represents the sample
 304 absorbance with 1 mg/L pCBA addition.

Parameter	Units	Groundwater	Wastewater effluent
DOC	mg _c /L	0.50	8.5
pH	SU	8.1	7.6
NO ₃ ⁻	mg-N/L	1.2	1.7
NO ₂ ⁻	mg-N/L	0	0
Alkalinity	mg/L as CaCO ₃	150	70
UVA 254	cm ⁻¹	0.021	0.170

305
 306
 307 Table S11. $k'_{\text{pCBA, indirect}}$ ($k'_{\text{pCBA, indirect}} = k'_{\text{pCBA}} - k'_d$) values were experimentally determined for
 308 MPUV/NO₃⁻ irradiation (1000 mJ/cm²) of groundwater and wastewater effluent (Table S8). The
 309 equivalent H₂O₂ concentration needed to achieve the same $k'_{\text{pCBA, indirect}}$ values during LPUV
 310 exposure were theoretically determined using a steady-state kinetic model (Wols et al. 2013)⁷.

	$k'_{\text{pCBA, indirect}}$ (cm ² /mJ)	MPUV/NO ₃ ⁻ (mg-N/L)	LPUV/H ₂ O ₂ (mg/L)
Groundwater	3.02E-04	1.2	1.30
Wastewater effluent	1.45E-04	1.7	3.80

312
 313
 314
 315
 316
 317
 318
 319
 320

321
322
323
324
325

326 **7 References**

327

- 328 (1) Bolton, J. R.; Linden, K. G. Standardization of Methods for Fluence (UV Dose)
329 Determination in Bench-Scale UV Experiments. *J. Environ. Eng.* **2003**, *129* (3), 209–215.
- 330 (2) Bircher, K. Calculating UV Dose for UV/AOP Reactors Using Dose/Log as a Water-Quality
331 Metric. *IUVA News* **2015**, *17* (2), 19–24.
- 332 (3) Keen, O. S.; Love, N. G.; Linden, K. G. The Role of Effluent Nitrate in Trace Organic
333 Chemical Oxidation during UV Disinfection. *Water Res.* **2012**, *46* (16), 5224–5234.
334 <https://doi.org/10.1016/j.watres.2012.06.052>.
- 335 (4) Montgomery, D. C. *Design and Analysis of Experiments*, Eighth edition.; John Wiley &
336 Sons, Inc: Hoboken, NJ, 2013.
- 337 (5) McKay, G.; Dong, M. M.; Kleinman, J. L.; Mezyk, S. P.; Rosario-Ortiz, F. L. Temperature
338 Dependence of the Reaction between the Hydroxyl Radical and Organic Matter. *Environ.*
339 *Sci. Technol.* **2011**, *45* (16), 6932–6937. <https://doi.org/10.1021/es201363j>.
- 340 (6) Buxton, G. V.; Greenstock, C. L.; Helman, W. P.; Ross, A. B.; Tsang, W. Critical Review of
341 Rate Constants for Reactions of Hydrated Electrons Chemical Kinetic Data Base for
342 Combustion Chemistry. Part 3: Propane. *J. Phys. Chem. Ref. Data* **1988**, *17* (2), 513.
343 <https://doi.org/10.1063/1.555805>.
- 344 (7) Wols, B. A.; Hofman-Caris, C. H. M.; Harmsen, D. J. H.; Beerendonk, E. F. Degradation of
345 40 Selected Pharmaceuticals by UV/H₂O₂. *Water Res.* **2013**, *47* (15), 5876–5888.
346 <https://doi.org/10.1016/j.watres.2013.07.008>.
- 347